International Conference
Nuclear Energy for New Europe

Development of a Thermo-mechanical Model for DTT PFU

Patrik Tarfila
Reactor Engineering Division, Jožef Stefan Institute
Jamova cesta 39
1000, Ljubljana, Slovenia
patrik.tarfila@gmail.com

Oriol Costa Garrido, Boštjan Končar
Reactor Engineering Division, Jožef Stefan Institute
Jamova cesta 39
1000, Ljubljana, Slovenia
oriol.costa@ijs.si, bostjan.koncar@ijs.si

ABSTRACT

This paper presents the development of a thermo-mechanical model of the divertor plasma-facing units (PFUs) for the Divertor Tokamak Test (DTT) facility. A finite element based numerical simulation of the structural model of one PFU under steady-state regime is performed, representing an operating condition relevant to the magnetic equilibrium in which DTT will operate (single null (SN) scenario). In the simulation, the pressure and the structural temperature field obtained in previous thermo-hydraulic simulations are employed as input loads. The thermo-mechanical model of the PFU has been developed assuming elastic material properties with addition of ideal plasticity, and a mesh sensitivity is performed to select an accurate yet computationally efficient mesh. The results of the simulation represent relevant thermo-mechanical parameters such as displacements, stresses and deformations, and the integrity of the PFU is verified against structural design criteria (SDC-IC).

1 INTRODUCTION

The Divertor Tokamak Test (DTT) facility is a tokamak fusion reactor, which will be built in Frascati (Italy) [1]. Its main purpose is to develop a system for exhaust power and particles; the component used for this application is the divertor. In DTT, several divertor designs will be tested for different plasma configurations [2]. The ashes and waste particles need to be removed by divertor because they are contaminating the plasma and reducing its effectiveness. Therefore, the heat fluxes on the divertor are very high due to thin scrape-off-layer and several simulations are needed to verify the structural integrity and cooling effectiveness of the plasma facing units (PFU).

This paper is the continuation of last year's thermo-hydraulic simulations with a full computational fluid dynamics (CFD) model of the divertor PFU [3], from which the pressure and the temperature fields of the solid components are used as inputs for the work presented here.

The main objectives of this paper are to calculate displacements, stresses and strains in the selected geometry with finite element method (FEM) and to verify the results against the structural design criteria for in-vessel components (SDC-IC) [4].

2 PFU GEOMETRY MODEL

The computer aided design (CAD) model of PFU remained the same as in the thermo-hydraulic simulations [3], but the fluid and twisted tapes were excluded. The geometry consists of 5 solid domains and materials (see Figure 1):

- Mono-block (Tungsten - W)
- Copper ring (Copper - Cu)
- Pipe (Copper-Chromium-Zirconium - CuCrZr (Treatment B))
- Supports (Stainless steel - AISI 316L(N)-IG)
- Connection weld (Inconel - Alloy 625)

All material properties (elastic modulus, Poisson's ratio, thermal expansion coefficient and yield strength) are modeled as temperature dependent [5], since the heat fluxes are higher than 1 $\mathrm{MW\,m^{-2}}$.

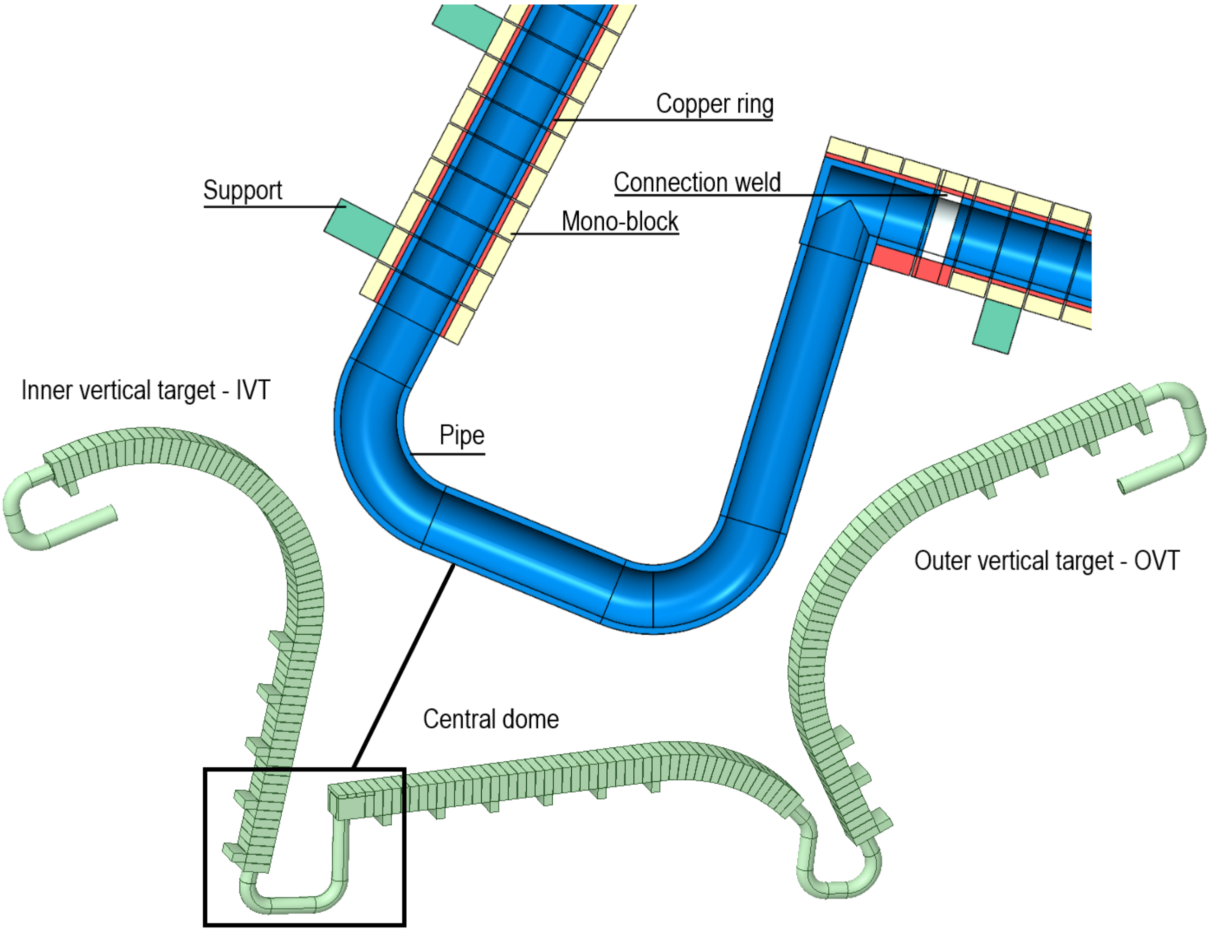

Figure 1: Geometry (bottom) and details of domains (top)

3 COMPUTATIONAL MODEL

Three-dimensional equations of thermo-elasticity were solved in the mesh sensitivity, with the addition of ideal plasticity for the copper in all other simulations. The FEM simulations were performed with the ABAQUS finite element code [6].

3.1 Model meshes

A mesh sensitivity was performed on the PFU model (Figure 1 bottom). Several meshes were used to check the stress convergence. Parameters and results are presented in Table 1. One parameter is the global size of finite elements (FE), which had an effect on the whole mesh. Second parameter is the number of FE through thickness of a copper ring, where the highest stress concentrations were expected.

Table 1: Mesh parameters and results

UNITS:	mm	/	MPa				/
MESH:	Elem. size	Num. of elem. through Cu ring	σ_{max}				Num. of elem.
	Global		M	C	P	S	
01	4	1	271.45	156.78	182.42	126.16	64907
02	1.25	1	324.08	149.75	241.67	145.87	677796
03	0.75	1	372.23	153.48	288.93	155.43	3218733
04	1.25	2	315.94	173.37	233.04	145.80	728489

Abbreviations: M = Mono-block, C = Copper ring, P = Pipe, S = Support

From Table 1 we can conclude that the mesh 04 (Figure 2a) is sufficient for the following reasons: the stresses in mono-block and pipe are still rising due to edge effect (Figure 2b) thus, comparing meshes 01-03, finer the mesh, higher are the stresses. The stresses in the support of mesh 04 are rather close to the very fine mesh 03. Stresses on the copper ring are higher in mesh 04 as compared to 02, because there are 2 FE through thickness instead of 1, hence 04 is more accurate.

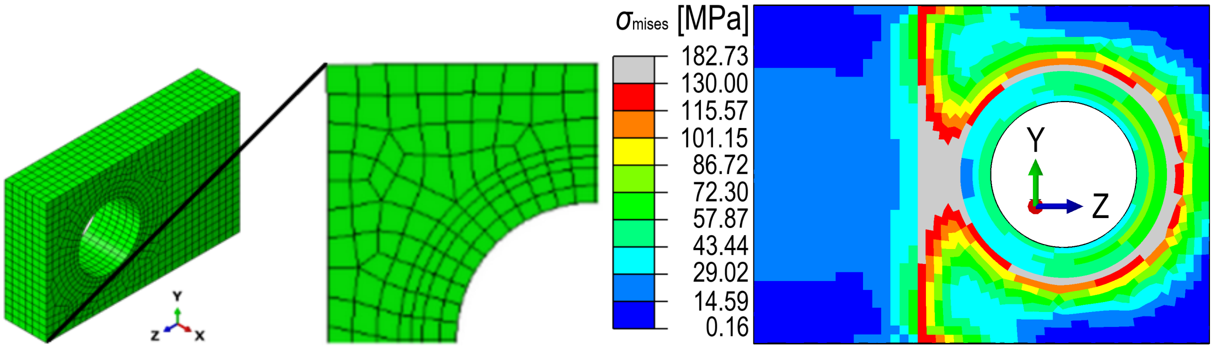

(a) The chosen mesh 04

(b) Edge effect on mesh 03

Figure 2: Mesh sensitivity results

3.2 Loads and boundary conditions

Two types of load were defined for the simulations. First is a pressure load of 5 MPa (see Figure 3 top-right). Second is the temperature field from thermo-hydraulic simulations [3] (see Figure 3), which was interpolated from finite volume to FE mesh using analytical mapped field in ABAQUS.

Boundary conditions (BC) were defined on the centerline of each support (green line in Figure 4 top-right) to allow support rotation. This centerline is blocked in the local z direction and supports 6, 12 and 13 are also fixed in local x direction. Inlet and outlet front faces are also blocked in x direction. All of the supports and inlet/outlet faces are also blocked in toroidal y direction on one vertex on the symmetry plane XZ (red points in Figure 4 center inset).

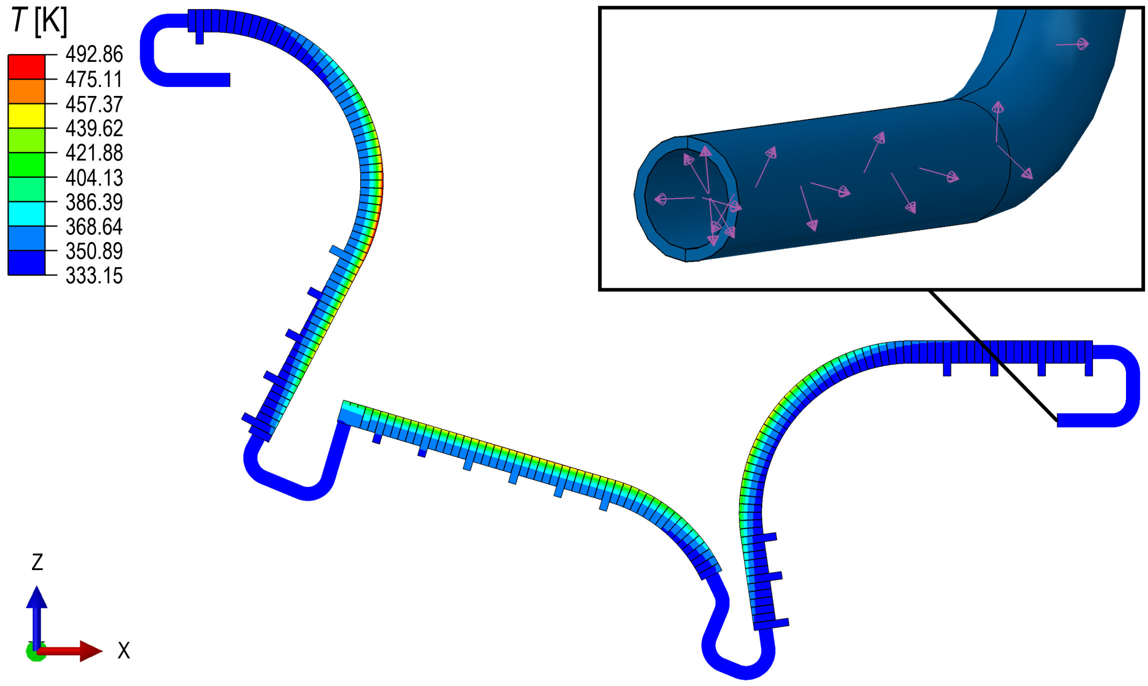

Figure 3: Temperature and pressure load

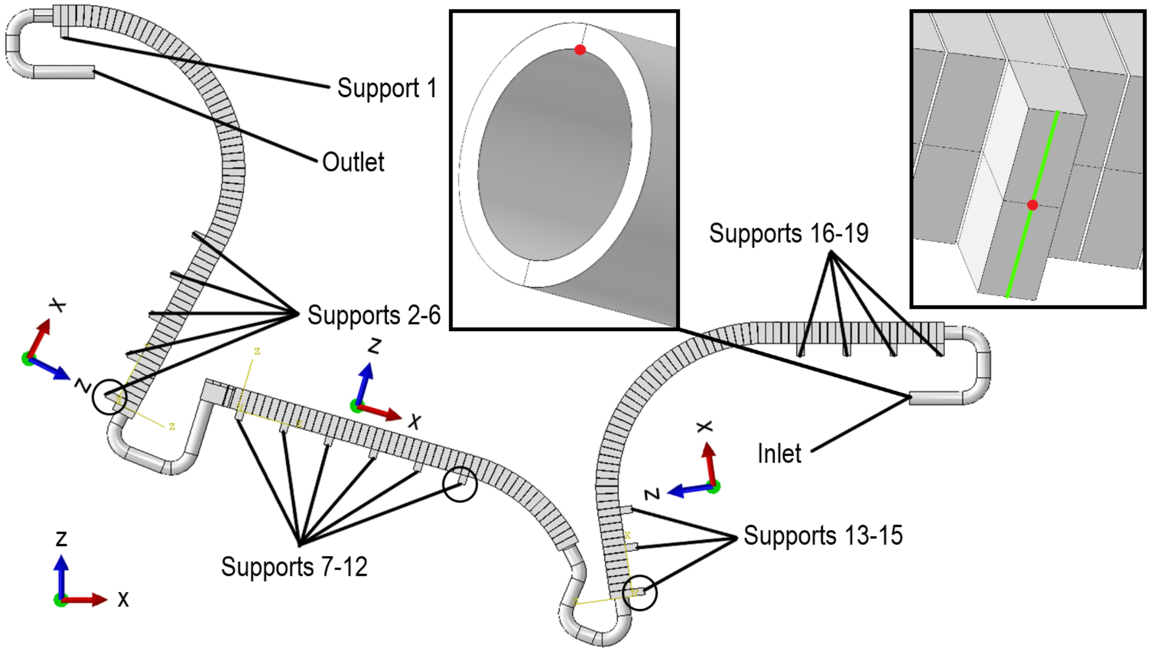

Figure 4: Boundary conditions

4 STRUCTURAL INTEGRITY ASSESSMENT

The results of thermo-mechanical simulations at most loaded (selected) locations are employed together with the design rules for fusion reactors to evaluate the component structural integrity. To that end, we performed calculations following the Structural Design Criteria for In-vessel Components (SDC-IC) [4]. Those criteria thus ensure that the required safety margins against different types of mechanical damage are fulfilled. The rules are split into 2 parts: elastic and elasto-plastic.

4.1 Elastic region

In this region the yield strength of materials is not surpassed. Criteria are checked on the so-called supporting line segment, a line defined between 2 outside surfaces perpendicular to at least one of them (Figure 5a). Then a stress linearization on that line needs to be performed. The total stress is broken down into membrane (average) stress, bending (linear) stress and the rest is called non-linear stress (Figure 5b).

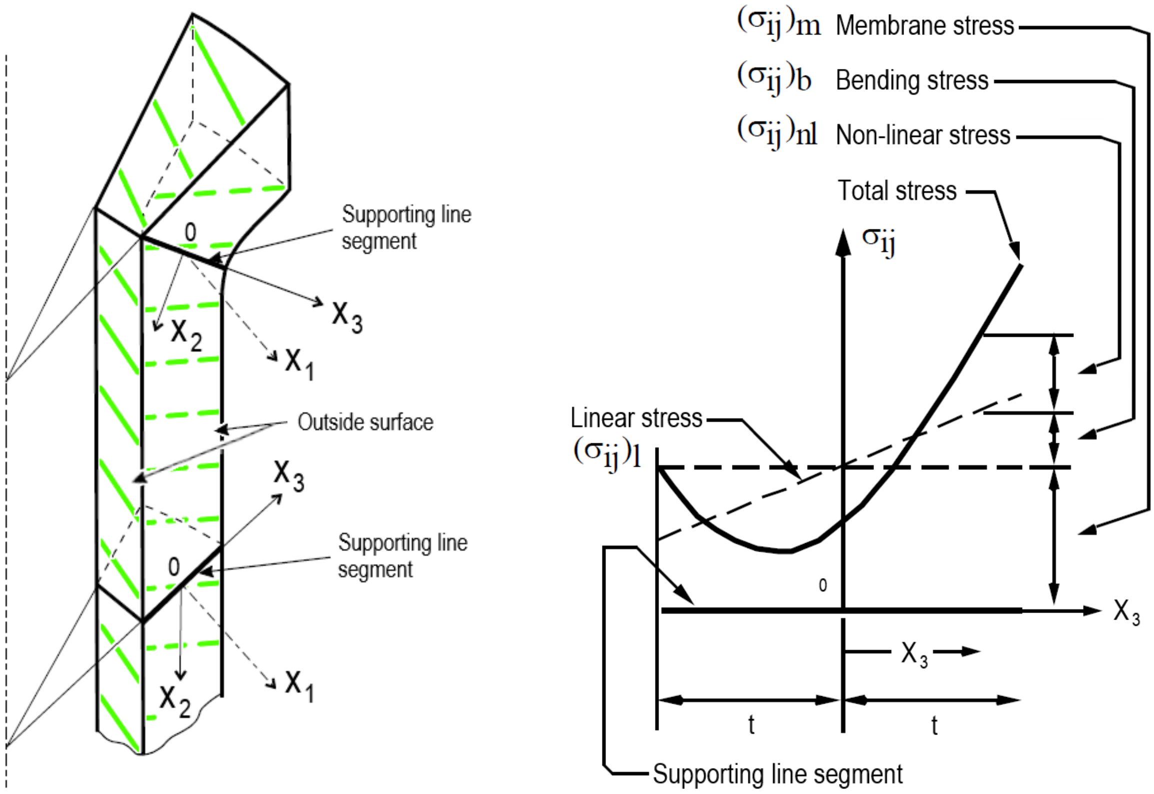

(a) Supporting line segment (summarized from [4]) (b) Stress linearization (summarized from [4])

Figure 5: SDC-IC code

The chosen criterion for elastic region is called a $3\,S_\mathrm{m}$ rule, which is represented with Eq. (1). This rule compares stresses in the component against an allowable stress. It includes local primary membrane stress P_L, primary bending stress P_b and local secondary stress Q_L. First two are the consequence of pressure and the last one is the consequence of temperature. Allowable primary membrane stress intensity S_m is defined as a fraction of yield or ultimate strength (material dependent).

$$\overline{P_\mathrm{L}+P_\mathrm{b}+Q_\mathrm{L}} \leq 3\,S_\mathrm{m} \tag{1}$$

4.2 Elasto-plastic region

For elasto-plastic region the variable is changed from stresses to strains, because the region is beyond its yield strength. Like in the elastic region, at first we perform a linearization, but on the strain tensor components. Then the principal stresses are calculated and the highest value is used for the chosen criterion, which is taking into account the immediate plastic flow localization (e.g. necking), defined with Eq. (2). The significant mean plastic strain $(\tilde{\varepsilon}_\mathrm{m})_\mathrm{pl}$ is the maximum principal strain of the plastic part of the strain tensor, and $\varepsilon_{\mathrm{u,\,min}}$ is the minimum uniform elongation, defined as the plastic component of the engineering strain when necking begins. To be able to apply this criterion, the thermo-mechanical simulation was run with required load factors, i.e. 2.5 and 1.5 on the pressure and temperatures respectively.

$$(\tilde{\varepsilon}_{\mathrm{m}})_{\mathrm{pl}} = \frac{\varepsilon_{\mathrm{u,\,min}}}{2} \tag{2}$$

5 RESULTS

After initial simulations with linear-elastic material properties, we concluded that for the components made from copper, the material should follow an elastic with ideal plasticity constitutive model due to very high stresses above yield. Therefore, the results assuming linear-elastic material properties in thermo-mechanical simulations are only be employed in the structural integrity assessment. Mises stresses are presented in Figure 6. The whole geometry is sectioned with XZ plane to show more details in the cross-section. The highest Mises stress is 258 MPa, located in the mono-blocks, and 171.32 MPa in the pipe, which is a structural component. Note that these values are taken from integration points, so there is some discrepancy with the extrapolated values in Figure. The detail in the middle of Figure 6 shows the radial stress σ_{rr} in cylindrical coordinate system. The stress at the inner surface of the pipe is equal to the pressure load of 5 MPa, as expected.

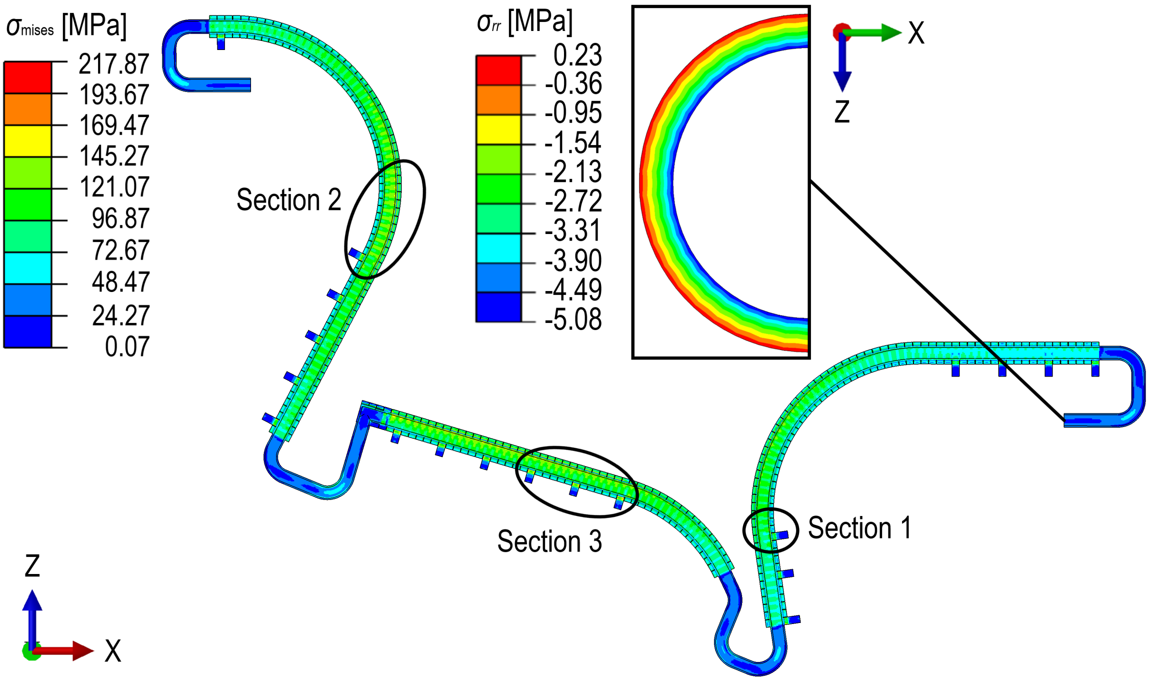

Figure 6: Mises stresses on the whole model with section view on XZ plane

As shown in Figure 7 at the top the displacements reach a maximum of 0.47 mm. The undeformed geometry is also added and the deformed geometry is scaled for a factor of 100. Most of the bending happens in the inner and outer vertical targets and a drift of geometry is present in the center dome. These parts are all very thermally loaded (Figure 3). The detail on the top right corner of Figure 7 also shows the rotation around supports, which was possible thanks to the modeling strategy presented Section in 3.2.

The distribution of equivalent plastic strain in copper components is shown at the bottom of Figure 7. Majority of copper rings were plastified, but the value of equivalent plastic strain is very low overall. The highest value of 3.8 % in the copper dome bend is very localized, and edges of copper rings reach about 0.86 % (also at the integration points).

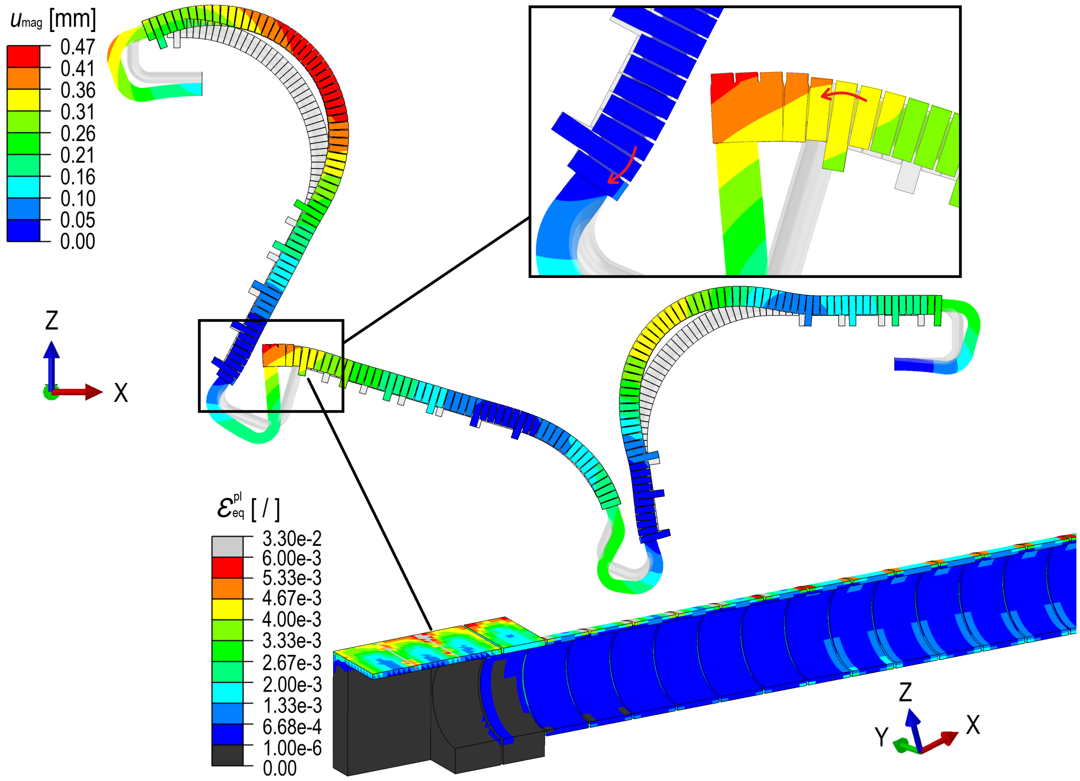

Figure 7: Displacements on the whole model (deformation scale factor 100) with undeformed geometry and equivalent plastic strain on copper parts

Structural integrity calculations of chosen criteria were performed with the results assuming elastic and elasto-plastic copper rings. For the elastic results 4 locations were selected: 2 for the pipe and 2 for the copper rings (Figure 8 left). For the elasto-plastic results 2 locations for the copper ring were selected (Figure 8 right). The 2 pipe locations correspond to the highest values of Mises stress and the copper ring locations represent average (1) and global maximum (2) stress/strain values. The detailed sections in Figure 8 are highlighted in Figure 6. The results of calculations are presented in Table 2. In elastic region, the stresses on the pipe are below the limit, so the pipe meets the criterion. In the copper rings, on the contrary, the stresses are over the limit even on the average level. The decision to use ideal plasticity for copper is now confirmed. In elasto-plastic region, the strains are below the limit even on the location of the global maximum equivalent plastic strain, so the copper rings now also meet the criterion.

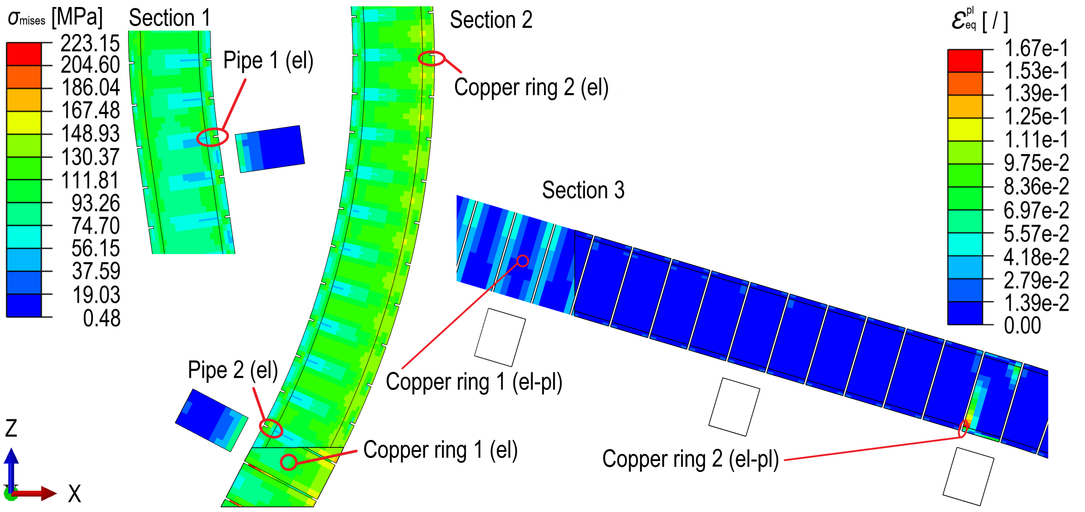

Figure 8: Locations of supporting line segments (elastic calculations left, elasto-plastic calculations right)

Table 2: Results from SDC-IC calculations

REGION:	Elastic					Elasto-plastic		
LOCATION:		Pipe		Cu ring			Cu ring	
		1	2	1	2		1	2
[°C], [°C]	T_{avg}	67.10	74.15	90.85	129.85	T_{avg}	267.65	246.65
RULE:	Eq. (1)					Eq. (2)		
[MPa], [/]	$\overline{P_{\mathrm{L}} + P_{\mathrm{b}} + Q_{\mathrm{L}}}$	181.94	185.88	120.59	197.46	$(\tilde{\varepsilon}_{\mathrm{m}})_{\mathrm{pl}}$	0.0041	0.0665
[MPa], [/]	$3\,S_{\mathrm{m}}$	369.00	369.00	91.10	86.42	$\varepsilon_{\mathrm{u,\,min}}$	0.1761	0.1822
	YES/NO	YES	YES	NO	NO	YES/NO	YES	YES

6 CONCLUSIONS

A thermo-mechanical simulation of one PFU was performed. The FE mesh was selected with a mesh sensitivity analysis. Loads were imported from previous thermo-hydraulic simulations and they correspond to the plasma SN scenario. The maximum stress of 258 MPa is in mono-block and the maximum displacement is 0.47 mm. Rotations around supports were successfully captured. Calculations following SDC-IC rules show that pipe in elastic region and copper rings in elasto-plastic region are below the limits with selected criteria.

ACKNOWLEDGEMENTS

This work has been carried out within the framework of the EUROfusion Consortium, funded by the European Union via the Euratom Research and Training Programme (Grant Agreement No. 101052200 - EUROfusion). Views and opinions expressed are however those of the author(s) only and do not necessarily reflect those of the European Union or the European Commission. Neither the European Union nor the European Commission can be held responsible for them. The financial support from the Slovenian Research Agency, grant P2-0405, is also gratefully acknowledged.

REFERENCES

[1] G. M. Polli, “Divertor Tokamak Testing Facility (DTT): A Test Facility for the Fusion Power Plant”, Paper presented at the OMC Med Energy Conference and Exhibition, Ravenna, Italy, September 2021. 978-88946678-0-6

[2] ENEA, Divertor Tokamak Test facility – Interim Design Report, (2019)

[3] P. Tarfila, B. Končar, O. C. Garrido, G. Dose, F. Giorgetti, and S. Roccella, “Development of a thermohydraulic model For DTT PFU,” in NENE 2022: 31st International Conference Nuclear Energy for New Europe, (2022), pp. 1012.1.-1012.8.

[4] Structural Design Criteria for In-vessel Components (SDC-IC), ITER, From Reactor Engineering Division R4 JSI collection, View date: 3.8.2022.

[5] ITER material properties handbook (Appendix A, Materials Design Limit Data). From Reactor Engineering Division R4 JSI collection, View date: 3.8.2022.

[6] Smith M. ABAQUS/Standard User’s Manual, Version 6.9. Providence, RI: Dassault Systèmes Simulia Corp, 2009.